

Available online at www.sciencedirect.com**ScienceDirect**

Procedia Engineering 120 (2015) 194 – 199

**Procedia
Engineering**www.elsevier.com/locate/procedia

EUROSENSORS 2015

Vacuum-packaged Resonant Pressure Sensor with Dual Resonators for High Sensitivity and Linearity

Bo Xie^a, Yonghao Xing^{a,b}, Yanshuang Wang^{a,b}, Deyong Chen^{b,*}, Junbo Wang^{b,†}^aUniversity of Chinese Academy of Sciences, Beijing 100190, China^bState Key Laboratory of Transducer Technology, Institute of Electronics, Chinese Academy of Sciences, Beijing 100190, China

Abstract

This paper presents a vacuum-packaged resonant pressure sensor featured with high sensitivity and linearity using dual resonators. The frequency difference between these two resonators is used to represent pressure, so that the nonlinear responds of each resonator is eliminated and the sensitivity of the sensor is also improved at the same time. The sensitivities of the dual resonators were matched through improved diaphragm uniformity and controlled anchor undercut, which led to a better linear performance. With this method, the nonlinear error is reduced from 1.3% F.S. to 0.2% F.S. over the pressure range from 0 to 250 kPa. Furthermore, to achieve better performance, the micro resonators were wafer-level vacuum packaged with anodic bonding to provide the needed low damping environment and the stable reference pressure. Test results show that the pressure in the vacuum-packaged micro chamber of the sensor is less than 5 Pa and kept for 6 months with no drop.

© 2015 Published by Elsevier Ltd. This is an open access article under the CC BY-NC-ND license (<http://creativecommons.org/licenses/by-nc-nd/4.0/>).

Peer-review under responsibility of the organizing committee of EUROSENSORS 2015

Keywords: resonant pressure sensor, dual resonators, high sensitivity and linearity, vacuum package;

1. Introduction

Resonant pressure sensors have better performances on the accuracy, stability, and reliability due to the quasi-digital output compared with the pressure sensors based on other mechanisms [1, 2]. This kind of sensors usually consists of a pressure sensitive diaphragm and a double-ends-clamped resonator. When pressure is applied to the

* Deyong Chen. Tel.: +86-10-58887182; fax: +86-10-58887182.

E-mail address: dychen@mail.ie.ac.cn

* Corresponding author. Tel.: +86-10-58887191; fax: +86-10-58887191.

E-mail address: jbwang@mail.ie.ac.cn

diaphragm of the sensor, it will be transferred into the inner stresses of the resonator, which results in the resonant frequency shift of the resonator. In order to improve the sensitivity, the diaphragm of the sensor is usually thinned. However, nonlinear error becomes another consideration when the diaphragm is hugely deflected under the high pressure just as other kinds of pressure sensors [3, 4].

To solve the contradiction between sensitivity and linearity, thinner diaphragm with centre boss [5] has been reported in piezoresistive pressure sensors. The centre boss on the diaphragm increases the stiffness of the diaphragm to avoid large deflection with slight reduction on the sensor's sensitivity. However, the accuracy was compromised due to the substantially increased acceleration sensitivity caused by the mass of centre boss, making it unsuitable for the resonant pressure sensor featured with high performance. Recently, the reported differential structure [6] can help the sensor to achieve better linearity and higher sensitivity without thinning the diaphragm thickness. However, the linear range is narrow, and the linearity improvement is limited due to the mismatched sensitivities of the dual resonators caused by the fabrication errors.

In this paper, a new electrostatically-driven resonant pressure sensor with two matched differential resonators was proposed. Two major improvements were implemented to match the sensitivities including the improved etching uniformity using a new hard mask of ZnO film and reduced undercut on the anchors by a self-made 2-step cycle processes. The linear working range was extended to a range from 0 to 250 kPa. Furthermore, the resonators were vacuum packaged with glass cap wafer using anodic bonding to improve the sensor's performance.

2. Sensor design and fabrication

2.1. Sensor design

The proposed micro sensor is based on a 4-inch SOI wafer for the convenience of the movable resonators. The triple layers of SOI are defined as different functions. The handle layer functioning as supporting layer is etched to form a pressure sensitive diaphragm. Two resonators on device layer are clamped on the diaphragm along the diagonal direction through the buried oxide layer. Each resonator is made of a doubly clamped resonant beam, a driving electrode, and a sensing electrode, which form two capacitors with parallel plate gaps of 2 μm . The beam is driven into lateral vibration by the electrostatic force between the plates of the driving capacitor, where squeeze film damping would be encountered. In order to reduce the damping, achieve the high Q-factor of the resonator, and provide the stable reference pressure, the resonators are vacuum packaged in a micro chamber with Pyrex 7740 glass cap wafer anodically bonded. Via holes are etched on the handle layer for the wire interconnections to the resonators. The schematic of the micro sensor is shown in Fig.1.

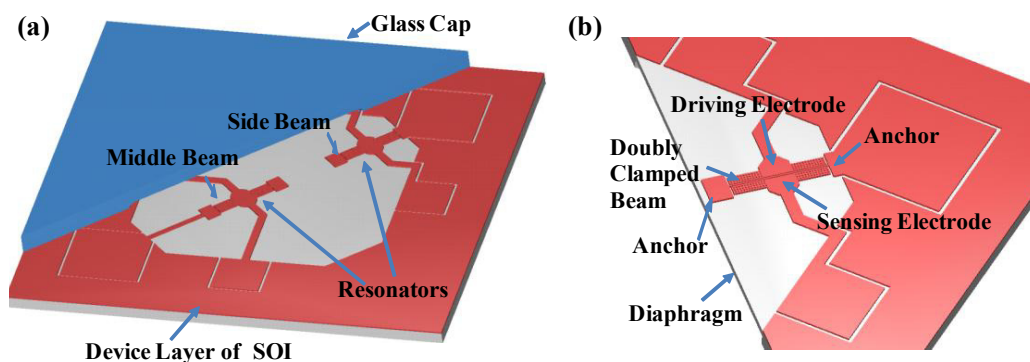


Fig. 1. (a) Top view of the proposed sensor with dual resonators packaged; (b) enlarged view of the resonator.

The two resonant beams are designed as a differential structure. The one near the central of diaphragm is named as “middle beam”, in which tensile stress would be encountered when pressure was applied to the diaphragm; while the other one named as “side beam” is subjected to the compile stress when under pressure. The tensile stress leads

to an increasing frequency shift of the middle beam, while the compress stress results in a decreasing frequency shift of the side beam. Thus, when the dual resonators have the same pressure sensitivities, the sensitivity of the sensor would be doubled with the frequency difference as represented the pressure. Besides, the nonlinear error of each resonator could be also reduced using the differential frequency as output. This method both improves the pressure sensitivity and reduces the nonlinear error without thinning the diaphragm, which will truly overcome the contradiction between sensitivity and linearity.

2.2. Fabrication

The fabrication of the micro sensor started with a 4-inch SOI wafer of a 40 μm device layer, a 2 μm buried oxide layer, and a 300 μm substrate layer. The wafer was heavily doped with a resistance of 0.001 to 0.005 $\text{ohm}\cdot\text{cm}$ for the reduction of capacitance feed-through [7]. The resonators were formed on the device layer using deep reactive ion etching. Then, diaphragms with a thickness of 120 μm and via holes of 300 μm deep were dry etched on the handle layer with multiple masks (see Fig. 2(b)). Afterwards, the resonators were released and the oxides in via holes were also removed as shown in Fig. 2(c). Then, the resonators were vacuum packaged with a glass cap wafer in bonding machine (SBe6, SUSS, German). Finally, the gold pads were maskless patterned in via holes using electrochemical etching with DC power applied to the handle layer. However, diaphragm thickness and anchor undercut seriously affected the sensitivity of each resonator, leading to the mismatching of the dual pressure sensitivities. Thus, the fabrication processes in Fig. 2 (b) and (c) should be further improved.

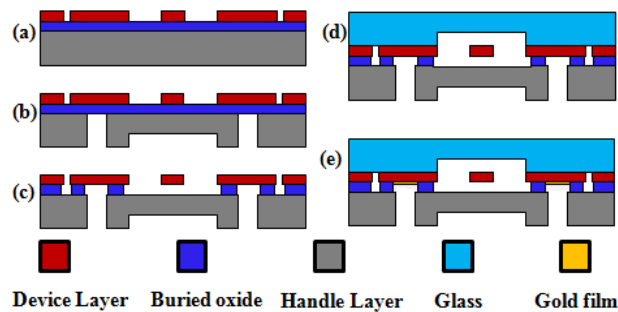


Fig. 2. The simplified fabrication flows of the proposed resonant pressure sensor.

In order to acquire the uniform diaphragm thickness, different mask materials including photo-resist, Al, and ZnO film were tried. The etching profiles are shown in Fig. 3. Photoresists of several micrometers are usually needed to achieve an etching depth of hundreds of micrometers due to the low selectivity to silicon [8]. The thick resist led to an uneven bottom with a variation of about 10 μm in our experiments, as shown in Fig. 3 (a) and (d). It was caused by the charge accumulation in the dielectric during the dry etching process. Although metal masks like Al film mitigated the problem of charge accumulation and greatly improved the selectivity to silicon, “micro masks” were always produced at the bottom making it unusable (see Fig. 3 (b)). A new hard mask of ZnO film was tried. The selectivity to silicon can be more than 1000:1 using a film of 1000 \AA to achieve an etching depth of 100 μm in Fig. 3 (c). Besides, a uniform bottom was also achieved with only a deviation of $\pm 1\mu\text{m}$, as shown in Fig. 3 (e).

To control the anchor undercut depth in the process of resonator releasing, a self-made vapor HF releasing processes were adopted. The releasing processes were consist of a series of 2-step cycle processes including vapor HF etching and water removal with isopropyl alcohol (IPA) steam. The schematic is shown in Fig. 4. The micro fabricated SOI wafer was firstly hung on a PTFE container with HF solution for 90s. The spontaneously evaporated HF steam was used to etch the exposed silicon oxide. It is worthy of mentioning that water accumulation should be avoided, because the produced water has a huge influence on the etching rate and the depth of undercut. To eliminate the influence, the wafer was then moved to another container with isopropyl alcohol (IPA) to remove the produced moisture and get the wafer dried. The IPA was adopted because of its strong volatility and affinity with

water. Besides, the adsorbed IPA molecules on silicon oxide also catalyzed the ionization of HF [9], which increased the etching rate of silicon oxide. Repeat the processes mentioned above until the resonant beams were movable when tested by the stepper (Alpha-step IQ, USA).

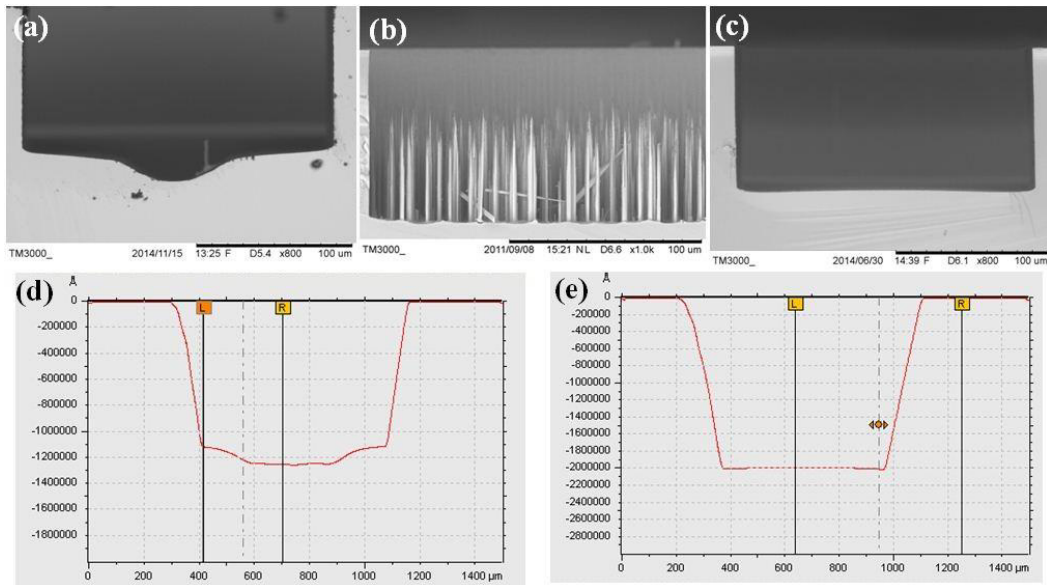


Fig. 3. The etching results with different masks. (a) and (d) Z4620 (4 μm); (b) Al (100 nm); (c) and (e) ZnO (100 nm).

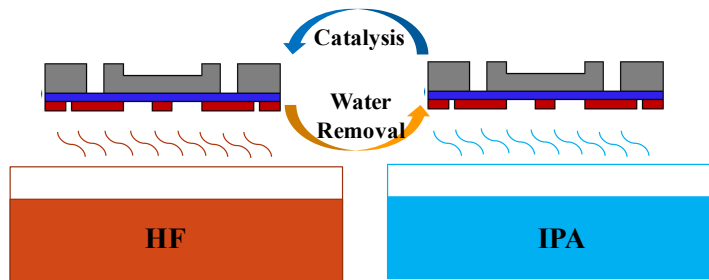


Fig. 4. Releasing the resonators with the proposed the 2-step cycle processes

The processes of etching silicon oxide proposed above were asynchronous, which means the two sides of SOI wafer were separately etched with different time. To remove the 2 μm oxide in holes, several cycles were enough according to the estimated etching rate. The etching results were shown in Fig. 5. Without water removal, the lateral etching was much faster than the vertical etching, leading to slope morphology, as shown in Fig. 5 (a) and (b). The undercut was about 10 times bigger than the thickness of oxide. Besides, the depths of undercut were also inconsistent with via hole varied. However, using the proposed 2-step processes, an isotropic etching with an undercut of about 2 μm was achieved as shown in Fig. 5 (c). While, to release the resonant beam with a width of 20 μm , dozens of cycles were needed where an undercut of 9 μm on the anchor was found in Fig. 5 (d). The undercut was minimized to the least value of half of the beam width, which was about 7 times smaller compared with the undercut in buffered HF caused by the two narrow gaps of 2 μm beside the beam.

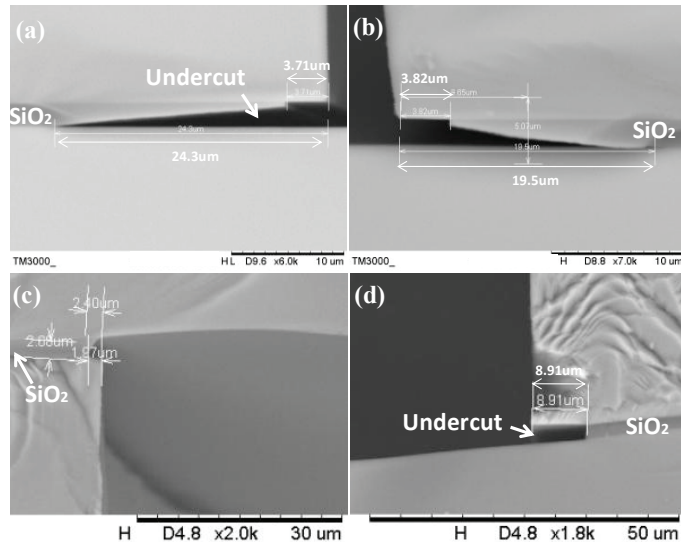


Fig. 5. The etching results with Vapor HF. (a) and (b) are the SEM image of removing SiO₂ in via holes without water removal; (c) is the SEM image of removing SiO₂ in via holes with the 2-step cycle process; (d) shows the release of the resonator using the 2-step cycle process, the undercut on the anchor was limited in 10 μm.

3. Sensor Characterization

The packaged pressure in the micro chamber of the proposed micro sensor was estimated by the Q-factor of the resonant beam. Fig. 6 (a) presents the results performed on a MEMS resonator before and after wafer-level packaging, showing that the pressure in the micro chamber is around 5 Pa. In order to test the reliability of the package, the Q-factor of micro sensor was intermittently tested for 6 months as shown in Fig. 6 (b). The Q-factor varied with time because of the temperature changing, but had no obvious drop and was kept in the order of ten thousand for more than 6 months. The test result indicates that a reliable packaging without leakage is achieved.

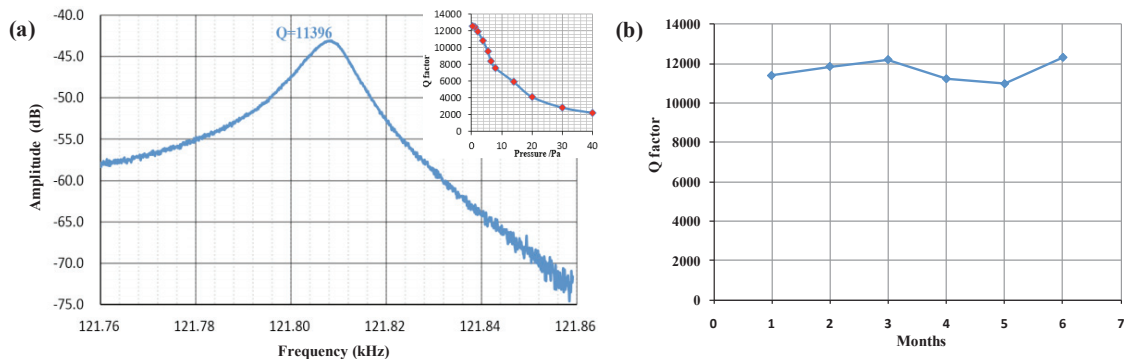


Fig. 6. (a) The Q-factor of the micro fabricated sensor is more than 10000, which indicates the vacuum achieved in the micro chamber is less than 5Pa. (b) The constant Q-factor in the past 6 months indicates the reliability of vacuum packaging and interconnection.

The pressure characteristic of the micro sensor is shown in Fig. 7. The sensitivities of the dual resonators are respectively 79.1 Hz/kPa and -81.0 Hz/kPa with a mismatch rate of $\pm 1.25\%$. Using the different frequency to represent the pressure, the sensitivity is doubled with a value of 160 Hz/kPa and the linear correlation coefficient is

improved from 0.9995 to 0.999994 in the pressure range from 0 to 250 kPa, and the nonlinear error is reduced from 1.3% F.S. to 0.2% F.S.

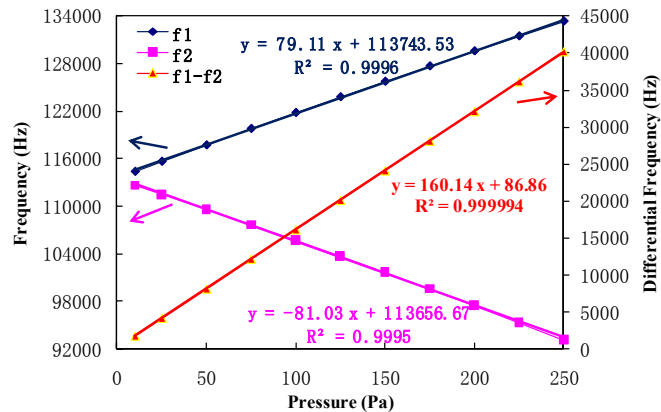


Fig. 7. The frequency responds of the resonators under applied pressure.

4. Conclusion

A reliable vacuum packaged resonant pressure sensor with dual resonators is fabricated to both improve the sensitivity and reduce the nonlinear error. The etching uniformity was improved with ZnO film as hard mask, and the undercut on anchor is reduced with a 2-step cycle process. Matched pressure sensitivities of 79.1 Hz/kPa and -81.0 Hz/kPa are achieved using the proposed fabrication processes. Using the dual resonators as differential structure, the sensitivity of the micro sensor is doubled with the nonlinearity error reduced from 1.3% F.S. to 0.2% F.S. in a wide range from 0 to 250 kPa.

Acknowledgements

This work is supported by the National Basic Research Program of China (Grant No. 2014CB744600), the National Sciences Foundation of China (Grant No. 61431019 and 61372054), and the National Key Foundation for Exploring Scientific Instrument (No.2013YQ12035703).

References

- [1] P.K. Kinnell; R. Craddock, Advances in Silicon Resonant Pressure Transducers, *Procedia Chemistry I*. 1 (2009) 104-107.
- [2] C.-F. Chiang; A.B. Graham; B.J. Lee; H.A. Chae; J. Ng. Eldwin; J. O'B. Gary; T.W. Kenny, *Micro Electro Mechanical Systems (MEMS), IEEE 26th International Conference on, Taipei, (2013) 45-48.*
- [3] Y. Zhang; R. Howver; B. Gogoi; N. Yazdi, A High-sensitive Ultra-thin MEMS Capacitive Pressure Sensor, *Solid-State Sensors, Actuators and Microsystems, 16th International Conference on, Beijing, (2011) 112-115.*
- [4] J.A. Chiou; S. Chen, Pressure Nonlinearity of Micromachined Piezoresistive Pressure Sensors with Thin Diaphragms under High Residual Stresses, *Sensors and Actuators A: Physical*. 147 (2008) 332-339.
- [5] J.A. Chiou; S. Chen, Structured Diaphragm with a Centre Boss and Four Peninsulas for High Sensitivity and High Linearity Pressure Sensors, *Micro & Nano Letters*. 9 (2014) 460-463.
- [6] Z.Y. Luo; D.Y. Chen; J.B. Wang; Y.N. Li; J. Chen, A High-Q Resonant Pressure Microsensor with Through-Glass Electrical Interconnections Based on Wafer-Level MEMS Vacuum Packaging, *Sensors*. 14 (2014) 24244-24257.
- [7] H.L. Jiao; B. Xie; J.B. Wang; D.Y. Chen; J. Chen, Electrostatically Driven and Capacitively Detected Differential Lateral Resonant Pressure Microsensor, *Micro & Nano Letters*. 8 (2013) 650-653.
- [8] K. Grigoras; L. Sainiemi; J. Tiilikainen; A. Säynätjoki; V.-M. Airaksinen; S. Franssila, Application of Ultra-thin Aluminum Oxide Etch Mask Made by Atomic Layer Deposition Technique, *J. Phys.: Conf. Ser.* 61 (2007) 369-373.
- [9] W.I. Jang; C.A. Choi; M.L. Lee; C.H. Jun; Y.T. Kim, Fabrication of MEMS Devices by Using Anhydrous HF Gas-phase Etching with Alcoholic Vapor, *J. Micromech. Microeng.* 12 (2002) 297-306.